CrossMark

CARDIAC

Diagnostic performance of calcification-suppressed coronary CT angiography using rapid kilovolt-switching dual-energy CT

Hiroto Yunaga[1] · Yasutoshi Ohta[1] · Yasuhiro Kaetsu[2] · Shinichiro Kitao[1] ·
Tomomi Watanabe[3] · Yoshiyuki Furuse[3] · Kazuhiro Yamamoto[3] · Toshihide Ogawa[1]

Abstract

Objectives Multi-detector-row computed tomography angiography (MDCTA) plays an important role in the assessment of patients with suspected coronary artery disease. However, MDCTA tends to overestimate stenosis in calcified coronary artery lesions. The aim of our study was to evaluate the diagnostic performance of calcification-suppressed material density (MD) images produced by using a single-detector single-source dual-energy computed tomography (ssDECT).

Methods We enrolled 67 patients with suspected or known coronary artery disease who underwent ssDECT with rapid kilovolt-switching (80 and 140 kVp). Coronary artery stenosis was evaluated on the basis of MD images and virtual monochromatic (VM) images. The diagnostic performance of the two methods for detecting coronary artery disease was compared with that of invasive coronary angiography as a reference standard.

Results We evaluated 239 calcified segments. In all the segments, the sensitivity, specificity, positive predictive value (PPV), negative predictive value (NPV) and accuracy for detecting significant stenosis were respectively 88%, 88%, 75%, 95% and 88% for the MD images, 91%, 71%, 56%, 95% and 77% for the VM images. PPV was significantly higher on the MD images than on the VM images ($P < 0.0001$).

Conclusions Calcification-suppressed MD images improved PPV and diagnostic performance for calcified coronary artery lesions.

Key Points
• *Computed tomography angiography tends to overestimate stenosis in calcified coronary artery.*
• *Dual-energy CT enables us to suppress calcification of coronary artery lesions.*
• *Calcification-suppressed material density imaging reduces false-positive diagnosis of calcified lesion.*

Abbreviations

AUC	Area under the receiver-operating characteristic curve
CAD	Coronary artery disease
CCTA	Coronary computed tomography angiography
CT	Computed tomography
ICA	Invasive coronary angiography
MD	Material density
MDCTA	Multi-detector-row computed tomography angiography
QCA	Quantitative coronary angiography
ROC	Receiver-operating characteristic
ssDECT	Single-detector single-source dual-energy computed tomography
VM	Virtual monochromatic

✉ Hiroto Yunaga
yunagahiroto@gmail.com

[1] Division of Radiology, Department of Pathophysiological Therapeutic Science, Faculty of Medicine, Tottori University, 36-1, Nishi-cho, Yonago City, Tottori 683-8504, Japan

[2] Department of Cardiology, Kakogawa Higashi Hospital, Kakogawa, Japan

[3] Division of Cardiology, Department of Molecular Medicine and Therapeutics, Faculty of Medicine, Tottori University, Yonago, Japan

Introduction

Coronary computed tomography (CT) angiography (CCTA) is a promising, minimally invasive method for detecting coronary artery stenosis in patients with suspected or known coronary artery disease (CAD) because of its high sensitivity and negative predictive value (NPV) [1–3].

The interpretation of CCTA images in the presence of coronary artery calcification is limited by partial volume averaging, which makes it difficult to clearly delineate between calcium deposits and the lumen [4, 5]. CCTA using single-energy CT can cause both overestimation and underestimation in the diagnosis of luminal stenosis and reduces diagnostic performance in patients with coronary calcification [6–11]. Recently, methods of eliminating the influence of calcification have been advocated, such as coronary calcium subtraction using a non-rigid registration approach with a 320-detector row CT scanner, virtual monochromatic (VM) images at high energy levels such as a 140-keV VM image obtained by dual-energy CT (DECT) and 200-keV VM image obtained by spectral CT [12–14].

Single-detector single-source dual-energy CT (ssDECT) acquires spatially matched raw data sets. These raw data are transformed into the densities of two selected basis materials and are able to generate material decomposition images by using two material decomposition methods [15]. Calcification-suppressed iodine material density (MD) images are created by decomposing calcium and iodine. These images are expected to improve the diagnostic performance of CCTA in cases of calcified lesions, but the validity of this method has not been established. The aim of our study was to evaluate the diagnostic performance of calcification suppressed MD images produced using ssDECT for calcified coronary artery lesions by comparing these images with VM images that have equal image quality to that of conventional single-energy CT images.

Materials and methods

Subjects

During an 18-month period, 372 patients with suspected or known CAD underwent CCTA at a single institution. Patients whose heart rates were faster than 60 beats per minute and had no contraindications to beta-blockers were pretreated with an oral beta-blocker (metoprolol 20 mg) 1 h before the scan. All patients received sublingual nitroglycerin. By using a single-energy helical scan instead, we examined 216 patients whose heart rates were faster than 60 beats per minute despite the use of beta-blockers or who had arrhythmias before the scan. The remaining 156 patients were examined by using a dual-energy axial scanner. Of these patients, 67 underwent coronary angiography if obstructive CAD was suspected on routine CCTA or if another medical test suggested ischemia (e.g. electrocardiography, myocardial stress scintigraphy and wall motion asynergy on echocardiography), as determined by the attending physician. All of the 67 patients were included in the study. This retrospective study protocol was approved by our institutional review committee, and written informed consent was obtained from all subjects.

CT protocol

All CT images were obtained by using single-source rapid kilovolt-switching dual-energy CT. Rapid kilovolt-switching is a type of acquisition in which a single-photon source alternates between two different X-ray energy levels (80 and 140 kVp) during gantry rotation [16]. Dual-energy acquisition with a prospective electrocardiogram-gated axial scan (SnapShot Pulse; GE healthcare) was used. As this axial scanning method was not suitable for patients with higher heart rates or arrhythmias in consequence of half reconstruction, only patients with a heart rate of at most 60 beats per minute were assessed using this method. Other scanning parameters used were as follows: tube current, 600 mA; rotation time, 350 ms; collimation, 0.625 mm × 64; display field of view, 180 × 180 mm; matrix, 512 × 512. The scan starting time was determined by using a test injection method, and image acquisition was started 2 s after the peak time. Iopamidol (370 mgI/mL, Iopamiron, Bayer, Osaka, Japan) was injected into the antecubital vein for 12 s at 12 mL/kg, followed by 25 mL of saline flush. Images were reconstructed at the most obvious resting point of the mid-diastolic phase. Adaptive statistical iterative reconstruction (ASiR, GE) by 50% was used for the 70-keV VM images. The ASiR could not be adapted to the iodine and hydroxyapatite pair MD image. So far, calcification-suppressed MD images were generated without iterative reconstructions.

Generation of VM and MD images

All of the collected data were transferred to a dedicated offline workstation (Advantage Workstation 4.6, GE), on which all images were generated. The principles of DECT are based largely on the photoelectric effect and can be achieved by exploiting the energy-dependent attenuation of materials when exposed to two different photon energy levels. These physical principles can be exploited for in vivo human imaging because DECT is based on dissimilar tissue characteristics with respect to their energy-dependent X-ray attenuation [13, 15]. Subsequently, DECT enables the distinct differentiation between two basis materials. These materials can be chosen arbitrarily, as long as their K edges are sufficiently different, such as water and iodine. VM images at any arbitrary energy from 40 to 140 keV can be created by using iodine and water

as the basis material pair. Each VM image depicted how the imaged object would appear if the X-ray source emitted only monochromatic X-ray photons [17]. We can instantly change between MD images and VM images at a workstation using a raw data set by selecting for image appearance, and we can simultaneously evaluate stenosis of calcified coronary arteries using MD images as well as non-calcified segments using VM images. As hydroxyapatite has been shown to be the major component of the ashing remnants of atherosclerotic plaques, by using hydroxyapatite and iodine as the basis material pair, a calcification-suppressed iodine density image can be generated [18]. In this study, as the CT numbers of the 60- to 80-keV VM images were close to those of the single-energy CT images and the highest contrast-to-noise ratio was obtained on the 68-keV VM images, the 70-keV VM images were adopted for comparisons with the single-energy acquisition CT images [19, 20].

CT image analysis

An 18-segment classification model was applied for image analysis [21]. After the segments with diameters less than 2 mm or treated by percutaneous coronary intervention were excluded, 457 segments were obtained. We eliminated 209 non-calcified segments on the VM images and evaluated 248 segments on the VM images. We also excluded nine segments because of image quality. The nine segments were in small branches, such as the distal left anterior descending or diagonal arteries, and had both poor VM image and MD image quality. Finally, the remaining 239 segments were analysed for diagnostic performance (Fig. 1). To avoid recall bias, the MD images were evaluated more than 3 months after the VM images were evaluated. The evaluated points were the extent of segment calcification, quality of MD images, residual calcification on MD images and luminal stenosis. We evaluated all segments visually on either curved multiplanar reformatted or stretched view images. The greatest
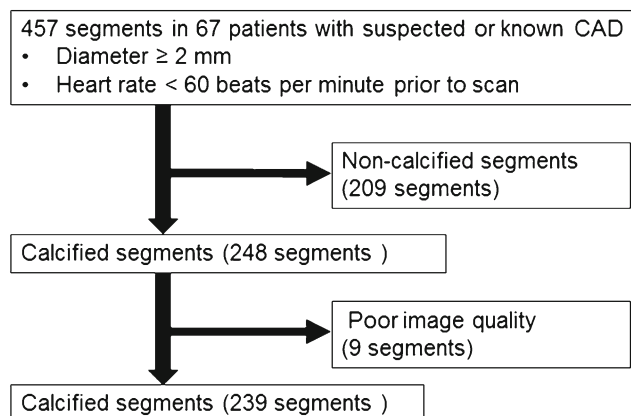
circumferential extent of calcification within the coronary segment (arc calcification) was assessed in all segments as follows: mild (0–90°), moderate (90–180°) and severe (greater than 180°) [10]. We classified the quality of the MD images into excellent, good, fair and poor (Fig. 2). Excellent was image quality without artefacts; good, with some artefacts present but interpretation was possible; fair, with moderate artefacts limiting adequate evaluation of the segment; and poor, made evaluation impossible. We classified the degrees of residual arterial calcification on MD images into three groups. Definition of residual calcification was as follows: none, no residual calcification was visually identified; obscure, partial hyperattenuation area of residual calcification was observed; unsuppressed, calcification was more remarkable than that observed on 70-keV VM images (Fig. 3). As quantitative assessment of luminal stenosis on MD images could not be performed on a dedicated workstation, luminal stenosis was assessed semiquantitatively both on MD images and VM images on the basis of the following criteria: minimal, less than 25% stenosis; mild, 25–49%; moderate, 50–69%; severe, greater than 70%; and occluded [21]. Two radiologists independently evaluated all the segments. One physician had more than 6 years of experience in cardiovascular radiology, and the other was a senior radiological resident with 2 years of experience in cardiovascular radiology. We considered segments with greater than 50% stenosis to be representative of significant stenosis. If a segment was classified as occluded, the distal segment of the vessel was considered to be an occluded segment. If discrepancies existed between the two observers, a consensus was achieved in discussion with a third reader after both reading sessions were completed. The diagnostic performance for detecting CAD (greater than 50% luminal diameter stenosis) was compared with that of invasive coronary angiography (ICA), which served as a reference standard.

Invasive coronary angiography

We performed ICA by using standard transfemoral or transradial arterial catheterization within 3 weeks after CCTA. A minimum of eight projections were obtained. An experienced cardiologist blinded to the CCTA results interpreted all the ICA images.

Quantitative coronary angiography (QCA) was performed by using an edge-detection algorithm with validated commercially available software (QAngioXA, Medis Medical Imaging Systems BV, Leiden, the Netherlands). The minimum lumen diameter in diastole or near the diastolic phase was measured from orthogonal projections. Any segments deemed visually to have greater than 15% stenosis were quantified. We deemed segments distal to total occlusions with incomplete contrast filling to be 100% occluded. QCA coronary artery segments were evaluated by using the same 18-

Fig. 1 Flow diagram of the reviewing process. *CAD* coronary artery disease

Fig. 2 Examples of image quality of material density (MD) images. The image quality of each segment of the MD images is classified into excellent (**a**), good (**b**), fair (**c**) and poor (**d**)

Excellent   **Good**   **Fair**   **Poor**
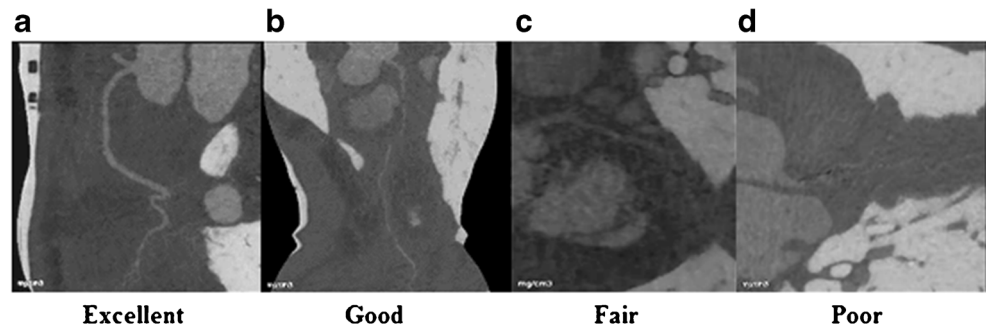
segment model used for CCTA. Lesions that caused greater than 50% occlusion of the lumen were considered as obstructive.

Radiation dose estimation was based on the dose–length product provided by the scanner for each patient and by using a correction factor of 0.014 for chest imaging in adults [22].

Statistical analysis

Statistical analyses were performed with commercially available software (SPSS version 17.0, IBM, Il, USA). For all continuous parameters, data were presented as mean ± SD. Sensitivity, specificity, positive predictive value (PPV), NPV and diagnostic accuracy were calculated by using standard methods [23]. Sensitivity and specificity were compared by using McNemar's test, and PPV and NPV were compared by using the method reported by Leisenring that uses the DTComPair package (version 1.00) in the statistical package R (version 3.1.2) [24]. The area under the receiver-operating characteristic (ROC) curve (AUC) and the DeLong method were used to compare the prediction of coronary stenosis between the different methods [25]. Interobserver agreement was calculated by using Cohen's kappa statistic. All tests were two-tailed, and a P value of less than 0.05 was considered statistically significant.
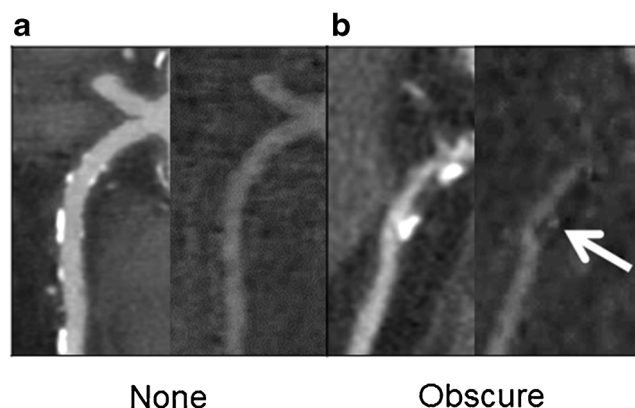

None   **Obscure**

Fig. 3 Classification of residual calcification on material density images. Of the images, 14% (33/239) showed obscure residual calcification, but blooming artefact is improved even in the obscure residual calcified segments (**b**)

Results

Patient characteristics

The characteristics of the 67 patients who underwent ssDECT are specified in Table 1. Of these patients, 50 were male and 22% (15/67) had a history of myocardial infarction. The mean heart rate was 57 beats per minute (range, 54–61 beats per minute). As patients with stents were included in this study, calcium scores were not calculated.

CT images

Of 239 calcified segments, 139 had mild calcification, 69 had moderate calcification and 31 had severe calcification. In total, 111 segments demonstrated excellent-quality MD images; 95, good; 33, fair.

Of the segments, 86% demonstrated no residual calcification on MD images, 14% were classified as obscure, and none was classified as unsuppressed (Table 2). Examples of each residual calcification rating are shown in Fig. 3.

Diagnostic performance

For all calcified segments, the sensitivity, specificity, PPV, NPV and accuracy were 91.3% (95% confidence interval [CI], 82.0–96.7), 70.6% (63.1–77.3), 55.8% (46.1–65.1), 95.2% (89.9–98.2) and 76.6% (70.7–81.8), respectively, on VM images, and 88.4% (78.4–94.9), 88.2% (82.4–92.7), 75.3% (64.5%–84.2%), 94.9% (90.3–97.8) and 88.3% (83.5–92.1), respectively, on MD images. False-positive diagnoses were reduced, and PPV was significantly improved on the MD images compared with that on the VM image. Other detailed diagnostic performance parameters for each degree of residual calcifications are shown in Table 3. The specificities for moderate and severe calcification significantly improved on the MD images (moderate calcification, $P < 0.0001$; severe calcification, $P = 0.025$). The PPVs for moderate and severe calcifications were more significantly improved on the MD images than on the VM images (moderate calcification, $P < 0.0001$; severe calcification, $P = 0.047$). Furthermore, the accuracies of the MD images were significantly improved for

Table 1 Patient characteristics ($n = 67$)

Male/female	50/17
Age (years)	72 (63–78)
Body mass index (kg/m^2)	23 (21–24)
Coronary risk factors	
Hypertension	45 (67)
Diabetes	26 (39)
Hyperlipidaemia	35 (52)
Smoking	30 (45)
Previous myocardial infarction	15 (22)
Multi-detector-row CT angiographic characteristics	
Heart rate (beats/min)	57 (53–61)

Values are presented as median (interquartile range) or n (%)

CT computed tomography

mild and moderate calcification ($P < 0.0001$ and $P < 0.0001$, respectively). The AUCs of the VM and MD images were respectively 0.892 (95% CI, 0.825–0.959) and 0.907 (0.841–0.972; $P = 0.658$) for mild calcification; 0.882 (0.798–0.966) and 0.976 (0.953–1.00; $P = 0.019$) for moderate calcification; 0.577 (0.373–0.782) and 0.793 (0.616–0.971; $P = 0.065$) for severe calcification; and 0.866 (0.818–0.914) and 0.922 (0.884–0.961; $P = 0.012$) for all segments (Fig. 4). Interobserver agreement was good to moderate ($\kappa = 0.656$) for the VM images and moderate ($\kappa = 0.573$) for the MD images. A representative case of a calcification-suppressed MD image is shown in Fig. 5. The estimated effective radiation dose of CCTA was 3.6 ± 0.1 mSv.

Discussion

Our study demonstrated that calcification-suppressed MD images were more useful than conventional CCTA images in the diagnosis of coronary artery stenosis in patients with calcified lesions on ssDECT.

Calcified coronary artery lesions often cause overestimation or underestimation [6–9]. The interpretation of CCTA images in the presence of coronary artery calcification is limited by partial volume averaging, which makes it difficult to clearly delineate between calcium deposits and the lumen [5]. Recently, methods of improving diagnostic performance for calcified coronary artery have been advocated, such as coronary calcium subtraction using a non-rigid registration approach with a 320-detector-row CT scanner [12], VM images at high energy levels such as 140 keV with DECT and 200 keV with spectral CT [13]. MD images produced using ssDECT make it possible to discriminate between two materials (e.g. iodine and hydroxyapatite) and provide a luminal iodine image that is less influenced by the presence of calcification. A recent report indicated that MD imaging using iodine and calcium as the basis material pair improved diagnostic performance for calcified coronary artery lesion in patients with high coronary calcium scores [26]. On the other hand, we used iodine and hydroxyapatite as the basis material pair in this study. As hydroxyapatite and calcium have different mass attenuation coefficients, calcification is suppressed differently between hydroxyapatite- and calcium-suppressed MD images. Consequently, hydroxyapatite- and calcium-suppressed MD images were visually quite different. Besides, sometimes a moderate or severe calcified coronary artery lesion is detected even if the calcium score is low, and the calcified lesion reduces the diagnostic performance. Furthermore, we investigated the diagnostic performance of MD images based on each coronary artery segment according to degree of calcification and found that calcification-suppressed MD images decreased the false-positive diagnosis of moderate or severe calcified coronary artery lesion.

The results of this technique were reduced rates of false-positive lesions on CCTA and improved PPV of calcified segments. The specificity and PPV of the calcification-suppressed MD images were better improved than those of the VM images. A statistically significant difference was found for moderate and severe calcification. We considered mild calcification to include spotty calcification that has less influence on luminal stenosis evaluation with VM images. Partial volume averaging did not have much influence on the evaluation of spotty calcified lesions, resulting in a non-significant improvement on MD images.

As hydroxyapatite has been shown to be the major component (99%) of calcified atherosclerotic plaques, we selected hydroxyapatite as the basis material when obtaining calcification-suppressed MD images [18]. The results indicated that 86% (206/239) of calcified coronary arteries demonstrated no signs of residual calcification. We suspected that

Table 2 Residual calcification on material density images

	Residual calcification none	Obscure	Unsuppressed	Overall
Degree of calcification				
Mild	126 (91)	13 (9)	0 (0)	139
Moderate	60 (87)	9 (13)	0 (0)	69
Severe	20 (65)	11 (35)	0 (0)	31
All	206 (86)	33 (14)	0 (0)	239

Values are presented as n (%)

Table 3 Degree of calcification and diagnostic performance of VM and MD images

Calcification	Image	Sensitivity	Specificity	Positive predictive value	Negative predictive value	Accuracy
Mild (n = 139)	VM	87.9 (29/33) [71.8–96.6]	83.0 (88/106) [74.5–89.6]	61.7 (29/47) [46.4–75.5]	95.7 (88/92) [89.2–98.8]	84.2 (117/139) [77.0–89.8]
	MD	84.8 (28/33) [68.1–94.9]	89.6 (95/106) [82.2–94.7]	71.8 (28/39) [55.1–85.0]	95.0 (95/100) [88.7–98.4]	88.5 (123/139) [82.0–93.3]
		P = 0.564	P = 0.052	P = 0.073	P = 0.704	P < 0.0001
Moderate (n = 69)	VM	93.8 (15/16) [69.8–99.8]	56.6 (30/53) [42.3–70.2]	39.5 (15/38) [24.0–56.6]	96.8 (30/31) [83.3–99.9]	65.2 (45/69) [52.8–76.3]
	MD	100 (16/16) [71.3–100]	90.6 (48/53) [79.3–96.9]	76.2 (16/21) [52.8–91.8]	100 (48/48) [89.1–100]	92.8 (64/69) [83.9–97.6]
		P = 0.317	P < 0.0001	P < 0.0001	P = 0.312	P < 0.0001
Severe (n = 31)	VM	95.0 (19/20) [75.1–99.9]	18.2 (2/11) [2.3–51.8]	67.9 (19/28) [47.6–84.1]	66.7 (2/3) [9.4–99.2]	67.7 (21/31) [48.6–83.3]
	MD	85.0 (17/20) [62.1–96.8]	63.6 (7/11) [30.8–89.1]	81.0 (17/21) [58.1–94.6]	70.0 (7/10) [34.8–93.3]	77.4 (24/31) [58.9–90.4]
		P = 0.317	P = 0.025	P = 0.047	P = 0.908	P = 0.237
All (n = 239)	VM	91.3 (63/69) [82.0–96.7]	70.6 (120/170) [63.1–77.3]	55.8 (63/113) [46.1–65.1]	95.2 (120/126) [89.9–98.2]	76.6 (183/239) [70.7–81.8]
	MD	88.4 (61/69) [78.4–94.9]	88.2 (150/170) [82.4–92.7]	75.3 (61/81) [64.5–84.2]	94.9 (150/158) [90.3–97.8]	88.3 (211/239) [83.5–92.1]
		P = 0.480	P < 0.0001	P < 0.0001	P = 0.874	P < 0.0001

Values are percentages (counts) [95% confidence interval] *VM* virtual monochromatic, *MD* material density

residual calcification occurred because of low spatial resolution or noise on MD images, or because the major component of the coronary artery calcification was a material other than hydroxyapatite (e.g. calcium oxalate) [27]. In either case, by reducing the partial volume effect, calcification-suppressed MD images improved diagnostic performance even if the calcification suppression was not perfect.

The concordance rate between the two observers for the MD images was less than that for the VM images. The appearance of the MD images was quite different from that of the VM images, so we presumed that the technique requires more practice before MD images can be of the same appearance as VM images.

The radiation dose used in rapid kilovolt-switching ssDECT was not twice the dose used in conventional CT. The dwell time was longer for the lower energy than the higher energy, and radiation dose values reach up to 20% higher for ssDECT than for conventional CT in the same patients [16]. Image acquisition using ssDECT has the following advantages: VM images correspond to various energies, beam-hardening correction and myocardial iodine quantification [20].

This study has some limitations. First, the population included previously treated patients, and the use of dual-energy axial scan was limited to patients with heart rates of at most 60 beats per minute because of its temporal resolution. Moreover, only patients in whom CCTA suggested obstructive CAD underwent ICA in this study. Therefore, obstructive CAD missed on CCTA might not have been noticed. To compensate for this drawback, we investigated diagnostic performance on a segment basis but could not do so on a patient basis. Although the purpose of our study was to investigate the usefulness of calcification-suppressed MD images for each degree of calcification in the coronary artery, further technical development is expected to adapt the technique to patients with higher heart rates and further investigation is needed to determine the usefulness of this method to reduce the number of patients undergoing ICA. Second, we used iodine and hydroxyapatite as the basis material pair, but residual calcification was observed in some segments. Materials other than hydroxyapatite should be investigated as components of calcified lesions to reduce residual calcification even further and to further improve the images obtained using this method. Third, as the purpose of our study was to compare diagnostic performance of MD images with single-energy CT for calcified coronary artery, we chose the 70-keV VM image equivalent to conventional 120-kVp CT image as the target for comparison. VM images at high energy levels have less blooming and beam-hardening artefact [28]. Thus, VM images at high energy levels might improve diagnostic performance for calcified coronary artery lesions [13]. A comparison of diagnostic performance between calcification-suppressed MD image and VM image at high energy levels is expected as a further examination. Fourth, CCTA quantification of lesion severity in terms of percentage maximal stenotic diameter has a good general correlation with quantitative ICA, and the inclusion of quantitative ranges with qualitative

Fig. 4 Area under the receiver-operating characteristic (ROC) curve (AUC) analysis of virtual monochromatic (VM) and material density (MD) images for each calcified coronary artery segment. ROC curves of VM and MD images for mild, moderate, severe, and all calcified segments
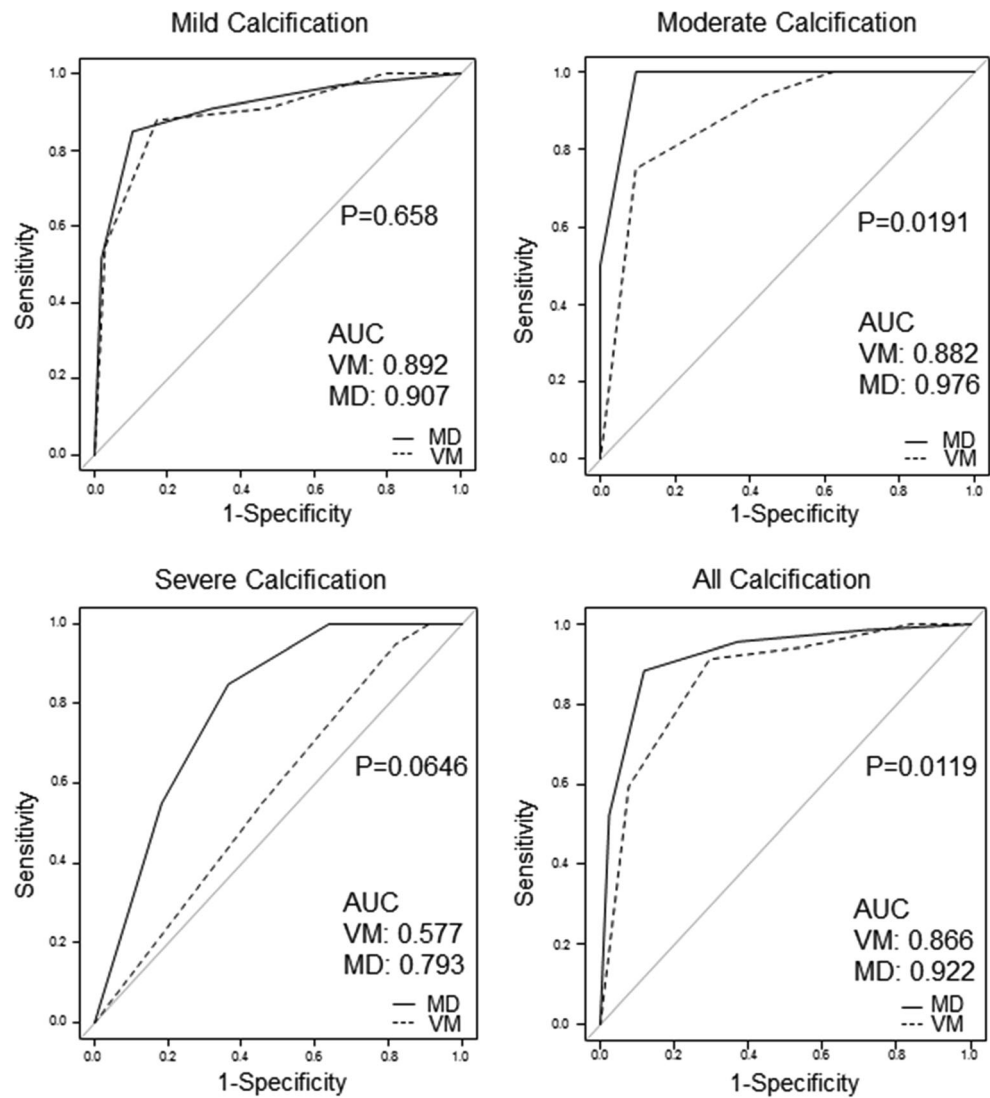
descriptions ensures that CCTA reporting is comparable to that using the traditional ICA lumen categories; this adds clarity to purely quantitative terms [21]. However, as no current software can quantitatively assess luminal stenosis in
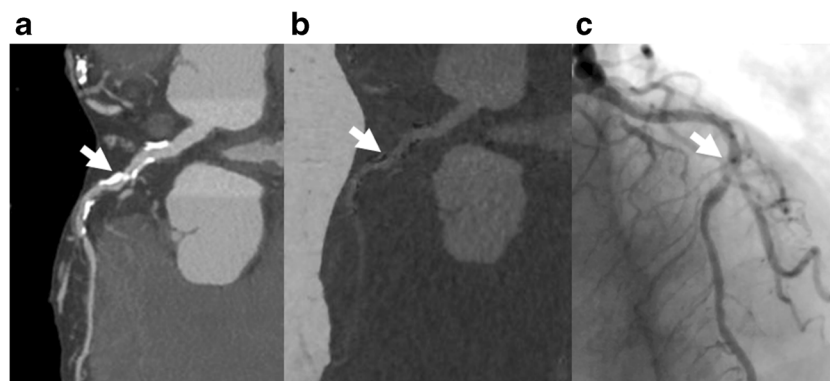
Fig. 5 Representative case of a conventional coronary computed tomography angiography (CCTA) image, a calcification-suppressed MD image and an invasive catheter angiography image. Coronary CT findings in a 92-year-old woman who presented with chest pain on exertion. The 70-keV conventional image shows a calcified obstructive lesion in the left anterior descending (LAD) artery (**a**). The calcification-suppressed MD image shows no obstructive lesion in the LAD artery, and no residual calcification is observed (**b**). The invasive coronary angiography (ICA) image shows no obstructive lesion in the LAD artery (**c**)

coronary artery lesions on MD images, we assessed luminal stenosis semiquantitatively. This is an important limitation, and requires further technical development.

In conclusion, calcification-suppressed MD images produced with ssDECT decreased the rate of false-positive results and increased the diagnostic performance for calcified coronary artery lesions in patients with relatively low heart rates.

References

1. Cordeiro MA, Miller JM, Schmidt A et al (2006) Non-invasive half millimetre 32 detector row computed tomography angiography accurately excludes significant stenoses in patients with advanced coronary artery disease and high calcium scores. Heart 92:589–597

2. Hamon M, Morello R, Riddell JW, Hamon M (2007) Coronary arteries: diagnostic performance of 16- versus 64-section spiral CT compared with invasive coronary angiography—meta-analysis. Radiology 245:720–731

3. Meijboom WB, Meijs MF, Schuijf JD et al (2008) Diagnostic accuracy of 64-slice computed tomography coronary angiography: a prospective, multicenter, multivendor study. J Am Coll Cardiol 52:2135–2144

4. Zheng M, Wei M, Wen D et al (2015) Transluminal attenuation gradient in coronary computed tomography angiography for determining stenosis severity of calcified coronary artery: a primary study with dual-source CT. Eur Radiol 25:1219–1228

5. Zhang S, Levin DC, Halpern EJ, Fischman D, Savage M, Walinsky P (2008) Accuracy of MDCT in assessing the degree of stenosis caused by calcified coronary artery plaques. AJR Am J Roentgenol 191:1676–1683

6. Budoff MJ, Dowe D, Jollis JG et al (2008) Diagnostic performance of 64-multidetector row coronary computed tomographic angiography for evaluation of coronary artery stenosis in individuals without known coronary artery disease: results from the prospective multicenter ACCURACY (Assessment by Coronary Computed Tomographic Angiography of Individuals Undergoing Invasive Coronary Angiography) trial. J Am Coll Cardiol 52:1724–1732

7. Ong TK, Chin SP, Liew CK et al (2006) Accuracy of 64-row multidetector computed tomography in detecting coronary artery disease in 134 symptomatic patients: influence of calcification. Am Heart J 151:e1–e6

8. Gottlieb I, Miller JM, Arbab-Zadeh A et al (2010) The absence of coronary calcification does not exclude obstructive coronary artery disease or the need for revascularization in patients referred for conventional coronary angiography. J Am Coll Cardiol 55:627–634

9. Arbab-Zadeh A, Miller JM, Rochitte CE et al (2012) Diagnostic accuracy of computed tomography coronary angiography according to pre-test probability of coronary artery disease and severity of coronary

arterial calcification. The CORE-64 (Coronary Artery Evaluation Using 64-Row Multidetector Computed Tomography Angiography) International Multicenter Study. J Am Coll Cardiol 59:379–387

10. Vavere AL, Arbab-Zadeh A, Rochitte CE et al (2011) Coronary artery stenoses: accuracy of 64-detector row CT angiography in segments with mild, moderate, or severe calcification—a subanalysis of the CORE-64 trial. Radiology 261:100–108

11. Yan RT, Miller JM, Rochitte CE et al (2013) Predictors of inaccurate coronary arterial stenosis assessment by CT angiography. J Am Coll Cardiol Img 6:963–972

12. Tanaka R, Yoshioka K, Muranaka K et al (2013) Improved evaluation of calcified segments on coronary CT angiography: a feasibility study of coronary calcium subtraction. Int J Cardiovasc Imaging 29:75–81

13. Danad I, Fayad ZA, Willemink MJ, Min JK (2015) New applications of cardiac computed tomography: dual energy, spectral, and molecular CT imaging. J Am Coll Cardiol Img 8:710–723

14. Vilades Medel D, Leta R, Alomar Serralach X, Carreras Costa F, Pons-Llado G (2016) Reliability of a new method for coronary artery calcium or metal subtraction by 320-row cardiac CT. Eur Radiol 26:3208–3214

15. Alvarez RE, Macovski A (1976) Energy-selective reconstructions in X-ray computerized tomography. Phys Med Biol 21:733–744

16. Silva AC, Morse BG, Hara AK, Paden RG, Hongo N, Pavlicek W (2011) Dual-energy (spectral) CT: applications in abdominal imaging. Radiographics 31:1031–1046

17. Pessis E, Campagna R, Sverzut JM et al (2013) Virtual monochromatic spectral imaging with fast kilovoltage switching: reduction of metal artifacts at CT. Radiographics 33:573–583

18. Hoffmann U, Kwait DC, Handwerker J, Chan R, Lamuraglia G, Brady TJ (2003) Vascular calcification in ex vivo carotid specimens: precision and accuracy of measurements with multidetector row CT. Radiology 229:375–381

19. Matsumoto K, Jinzaki M, Tanami Y, Ueno A, Yamada M, Kuribayashi S (2011) Virtual monochromatic spectral imaging with fast kilovoltage switching: improved image quality as compared with that obtained with conventional 120-kVp CT. Radiology 259:257–262

20. Scheske JA, O'Brien JM, Earls JP et al (2013) Coronary artery imaging with single-source rapid kilovolt peak-switching dual-energy CT. Radiology 268:702–709

21. Leipsic J, Abbara S, Achenbach S et al (2014) SCCT guidelines for the interpretation and reporting of coronary CT angiography: a report of the Society of Cardiovascular Computed Tomography Guidelines Committee. J Cardiovasc Comput Tomogr 8:342–358

22. Hausleiter J, Meyer T, Hermann F et al (2009) Estimated radiation dose associated with cardiac CT angiography. JAMA 301:500–507

23. Zou KH, O'Malley AJ, Mauri L (2007) Receiver-operating characteristic analysis for evaluating diagnostic tests and predictive models. Circulation 115:654–657

24. Leisenring W, Alonzo T, Pepe MS (2000) Comparisons of predictive values of binary medical diagnostic tests for paired designs. Biometrics 56:345–351

25. DeLong ER, DeLong DM, Clarke-Pearson DL (1988) Comparing the areas under two or more correlated receiver operating characteristic curves: a nonparametric approach. Biometrics 44:837–845

26. Andreini D, Pontone G, Mushtaq S et al (2015) Diagnostic accuracy of rapid kilovolt peak-switching dual-energy CT coronary angiography in patients with a high calcium score. J Am Coll Cardiol Img 8:746–748

27. Fishbein GA, Micheletti RG, Currier JS, Singer E, Fishbein MC (2008) Atherosclerotic oxalosis in coronary arteries. Cardiovasc Pathol 17:117–123

28. Mannelli L, MacDonald L, Mancini M et al (2015) Dual energy computed tomography quantification of carotid plaques calcification: comparison between monochromatic and polychromatic energies with pathology correlation. Eur Radiol 25:1238–1246